Journal of Power Sources 195 (2010) 1065–1070

Contents lists available at ScienceDirect

Journal of Power Sources

journal homepage: www.elsevier.com/locate/jpowsour

Short communication

Preparation of hollow carbon nanocages by iodine-assisted heat treatment

Shang Jun Teng[a], Xiao Xia Wang[b], Bao Yu Xia[a], Jian Nong Wang[b,*]

[a] Shanghai Key Laboratory for Laser Processing and Materials Modification, School of Materials Science and Engineering, Shanghai Jiao Tong University, 800 Dong Chuan Road, Shanghai 200240, PR China

[b] Shanghai Key Laboratory for Metallic Functional Materials, Key Laboratory for Advanced Civil Engineering Materials (Ministry of Education), School of Materials Science and Engineering, Tongji University, 1239 Siping Road, Shanghai 200092, PR China

ARTICLE INFO

Article history:
Received 7 July 2009
Received in revised form 26 August 2009
Accepted 26 August 2009
Available online 2 September 2009

Keywords:
Carbon nanocage
Iodine
Heat treatment
Platinum
Fuel cells

ABSTRACT

Carbon nanocages (CNCs) with a hollow structure and high degrees of graphitization and purity have wide applications. However, preparation of such material is still a great challenge. In this study, we report a general strategy for the preparation from iron/graphite core-shell nanoparticles. The core-shell nanoparticles are synthesized by the pyrolysis of acetylene with iron carbonyl. In order to remove the metallic core, rather than using the conventional acid oxidation, the nanoparticles are heat treated in the presence of iodine. It is found that the entrapped iron particles can be completely eliminated and hollow CNCs with good graphitization and high purity can be obtained. The purification process may involve the diffusion of iron atoms out from CNCs and their reaction with iodine molecules in the surrounding atmosphere. The reaction product FeI_2 is soluble in ethanol and could thus be easily removed. As an example of a potential application, the CNCs are demonstrated to be a superb material for supporting the Pt catalyst used in low-temperature fuel cells. The present method could be applied to the production of graphitic carbon in large scale, and the resultant material could prove to be practically relevant for fuel cell and many other technologies.

1. Introduction

Nanostructured graphitic carbon materials have well-developed crystalline structures, high electrical conductivity, good thermal stability and oxidation resistance at low temperature [1–4]. So they have potential applications in many fields such as adsorbents, energy-storage media, catalyst supports and electrode materials. Particularly, it has been proposed that carbon materials with a well graphitized structure can lead to a higher electrocatalytic activity and improved durability when used as a catalyst support compared with conventional amorphous carbon [5–7]. Carbon nanocages (CNCs) have a special hollow structure with graphitic shells and show excellent performance as a catalyst support in proton exchange membrane fuel cells (PEMFC) [8–11].

To date, some methods have been developed to prepare CNCs [8,9,12–15]. Chemical vapor deposition (CVD) is a widely employed technique due to its simplicity and high yield. This method involves the catalytic decomposition of molecules containing carbon atoms. The catalyst is generally transition metals (e.g. Fe) and the metal forms the core for the formation of external graphitic shells. In order to obtain hollow CNCs, it is necessary to remove the encapsulated metal particles.

At present, little attention has been paid for the removal of the metal particles encapsulated in the CNCs. Boiling in concentrated acid (HNO_3, H_2SO_4, HCl, etc.) is a generally used method [13,16–20]. But these acids have strong oxidation effects, which damage the graphitic structure and also cause significant loss of carbon materials during acid boiling. In addition, strong acids are less desirable for large-scale production because of high costs and environment concerns [16–18,21–23]. Furthermore, for those CNCs prepared at high temperature with a well-developed and thick graphitic structure, the entrapped metal particles cannot be removed because of the high resistance of the graphitic shells to acid oxidation [21–26].

In this paper, a novel method is reported for preparing hollow CNCs. First, iron/graphite core-shell nanoparticles were produced by the pyrolysis of a mixture of acetylene and iron carbonyl. Then, the core-shell nanoparticles were heat treated in the presence of iodine. Finally, they were mixed with ethanol and filtrated. As will be shown, the Fe particles entrapped by graphitic shells can be removed with little damage of the graphitic structure and little loss of carbon material and no acid is used. The hollow CNCs show improved electrochemical catalytic activity when used as a support material for Pt than CNCs obtained by acid processes.

* Corresponding author. Tel.: +86 21 65982867; fax: +86 21 65985385.
E-mail address: jnwang@tongji.edu.cn (J.N. Wang).

0378-7753/$ – see front matter © 2009 Elsevier B.V. All rights reserved.
doi:10.1016/j.jpowsour.2009.08.076

2. Experimental

2.1. Preparation of core-shell nanoparticles

The iron/graphite core-shell nanoparticles were prepared by a CVD approach. N_2–C_2H_2 mixed gases were flowed through the liquid iron carbonyl ($Fe(CO)_5$) and supplied into a quartz reactor heated at 1300 °C. N_2 was used as a carrier gas at a flow rate of 160 L h^{-1} and C_2H_2 as the carbon source at 40 mL min^{-1}. The prepared sample was collected in a glass bottle connected with the quartz reactor.

2.2. Removal of metal core

The as-prepared sample was mixed with excess iodine and placed at one end of a quartz tube. After the tube was evacuated and filled with N_2 to atmospheric pressure, it was heated at 1000 °C for 30 min. After cooling to ambient temperature, the heated sample was directly washed and filtered with ethanol for several times until the filtrate was transparent. The sample collected at the filter was dried at 80 °C for 3 h. For the purpose of comparison, the as-prepared sample was also refluxed in a mixed acid solution of HCl and HNO_3 with a volume ratio of 3:1 at 120 °C for 6 h. The treated solution was diluted with distilled water, and similarly filtrated, washed and dried.

2.3. Characterization of CNCs

X-ray diffractometer (XRD) was operated at 35 kV and 200 mA with nickel-filtered Cu-Kα radiation as an incident beam (D/max 2550VL/PC), to study the crystallization of carbon and other phases contained in the samples. Typical transmission electron microscopy (TEM) and high resolution transmission electron microscopy (HRTEM) with a cold field emission gun (JEOL-2010F, accelerating voltage of 200 kV) were used to investigate the microstructure and morphology of the sample. Nitrogen adsorption/desorption isotherms of CNC samples were measured at 77 K using a BELSORP instrument (BEL Inc., Japan). The sample was outgassed at 200 °C under nitrogen flow for 2 h prior to the measurement. The total surface area was calculated from the Brunauer–Emmett–Teller (BET) equation from the adsorption data in the relative pressure from 0.04 to 0.2. The mesopore size distribution (>2 nm) was determined by the Barrett–Joyner–Halenda (BJH) method and the micropore size distribution (<2 nm) was studied by micropore analysis method (MP method) [27]. Raman spectroscopy was carried out to examine the perfection of the hollow CNCs obtained from heat treatment with iodine using a Horiba Jobin Yvon HR 800UV with the 514.5 nm excitation wavelength laser.

2.4. Preparation of Pt/CNC catalyst and electrochemical activity

Pt/CNC catalysts were prepared by polyol reduction. The Pt loading on CNCs was 45 wt.%. At first, CNCs were sonicated in ethylene glycol to form slurry. Then, the slurry was heated up to around 140 °C. A chloroplatinic acid (CPA) solution, prepared by dissolving CPA (H_2PtCl_6) in ethylene glycol, was added slowly into the CNC slurry. The mixture was refluxed at 140 °C for 3 h. After cooling to room temperature, the catalyst was filtered, washed with distilled water and dried for the subsequent measurement. Glassy carbon (GC) (Bas electrode, 0.07 cm^2) was polished to a mirror with a 0.3 μm alumina powder suspension before each experiment and served as an underlying substrate of the working electrode. In order to prepare the composite electrode, the Pt/CNC catalyst was dispersed ultrasonically in the mixed solution of ethanol and 5 wt.% Nafion solution and 20 μl aliquot was transferred on to a polished glassy carbon substrate. The amount of Pt on the electrode was controlled to be 0.4 mg cm^{-2} on all electrodes. After the evaporation of ethanol, the resulting thin catalyst film was covered on the glassy carbon substrate. Then, the electrode was dried at room temperature and used as the working electrode. The electrochemical activities of the catalysts were characterized by cyclic voltammetry (CV). The experiments were performed using a three-electrode cell with an EG&G potentiostat (Model 366A) at ambient temperature and 0.5 M H_2SO_4 was used as the electrolyte.

3. Results

3.1. As-prepared core-shell nanoparticles

The as-prepared samples appeared as a black powder and the XRD pattern is illustrated in Fig. 1a. The peak at $2\theta = 26.1°$ could be attributed to diffraction from the (0 0 2) planes of the hexagonal structure of graphite. Those appearing at $2\theta = 44.6°$, 65.0° and 82.3° resulted from the diffractions of the (1 1 0), (2 0 0) and (2 1 1) planes of iron (Fe), and the rest peaks were related to the martensite [Fe, C] phase which was mainly composed of $Fe_{15.1}C$. The TEM image of the sample is shown in Fig. 1b. As can be seen, the sample consisted of well-dispersed nanoparticles with an average diameter of about 30–50 nm. Furthermore, each nanoparticle had an iron/graphite core-shell structure. The HRTEM image (Fig. 1c) confirmed the presence of an ordered crystalline structure in the shell of the particle and the thickness was about 5–10 nm, which was thicker than those prepared at low temperature [8–10].

3.2. CNCs after core removal

After heat treatment with iodine, the sample was examined by XRD, as shown in Fig. 2a. Besides the diffraction peaks for C and I_2, there are other peaks related to FeI_2. The original Fe or Fe–C phase could no longer be observed. In Fig. 2b, the peaks for FeI_2 and I_2 have disappeared, and there are only peaks of graphite after ethanol filtration. This result indicates that heat treatment with iodine followed by filtration by ethanol is an effective method to remove the Fe particles entrapped by well-developed graphitic shells. However, in the sample purified by conventional direct boiling in a mixed acid, the original Fe and Fe–C phase was still remained (Fig. 2c), illustrating that boiling in a strong acid was not a practical way to remove the Fe particles for the sample with a good graphitic shell structure.

Fig. 3 shows the TEM images of the sample after iodine treatment. It could be concluded that the Fe particles were removed completely using this method and hollow CNCs were obtained. The cage size was 30–50 nm in the outer diameter with the shell thickness being 5–10 nm (Fig. 3a), which is consistent with the as-prepared sample. HRTEM image illustrates that the cage shell was composed of about 20 well-defined graphitic layers with a spacing of 0.34 nm (Fig. 3b).

The graphitization of the present hollow CNCs can be further characterized by Raman spectroscopy (Fig. 4). The spectrum of the CNCs presents two peaks characteristic of the graphite structure at approximately 1350 and 1581 cm^{-1}, respectively. The peak at 1581 cm^{-1} can be identified as the G peak of the perfect crystalline graphite arising from the zone-center E_{2g} mode, and the peak at 1350 cm^{-1} as the D peak assigned to the A_{1g} zone-edge phonon induced by the disorder in the graphite lattice [24–26]. The relative high intensity ratio ($I_G/I_D = 1.9$) of the CNCs indicates that the graphitization of the present hollow CNCs remained quite good after heat treatment at 1000 °C.

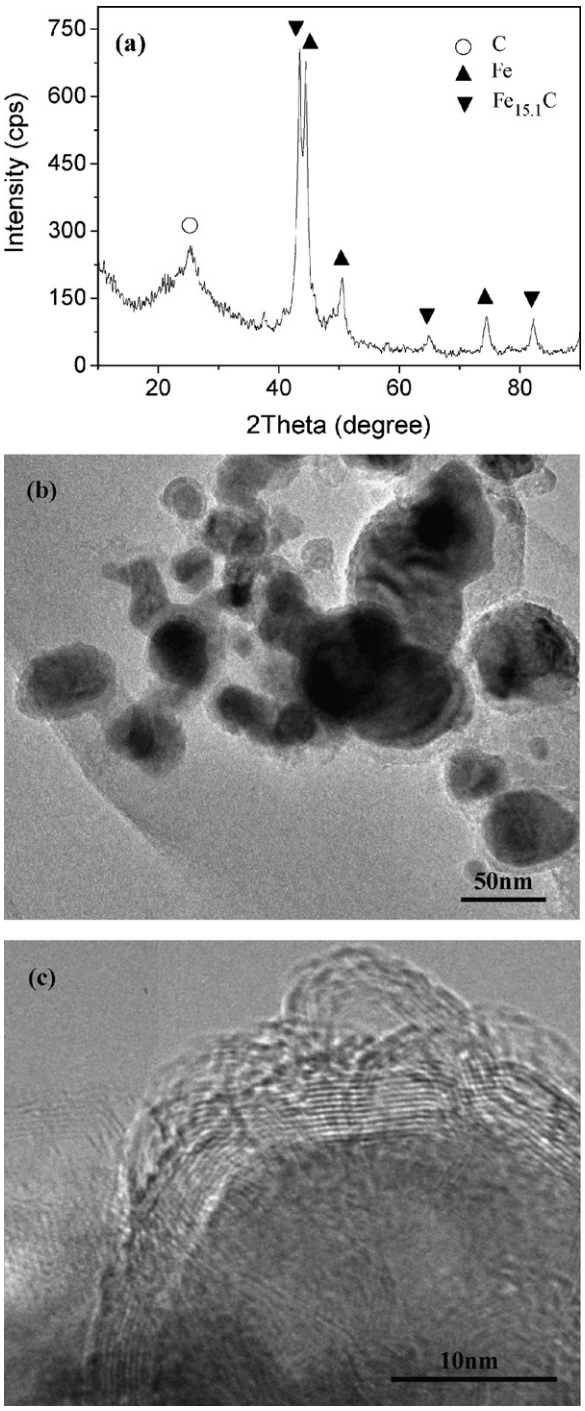

Fig. 1. XRD pattern (a), TEM image (b), and HRTEM image (c) of the as-prepared sample.

N_2 adsorption/desorption experiments were carried out to analyze the pore structures and the pore size distribution in the CNCs obtained by iodine treatment and acid treatment. As can be seen in Fig. 5a, the CNC samples exhibited typical IV isotherms with H1 hysteresis [28,29]. The obvious hysteresis of desorption for CNCs from iodine treatment between the partial pressures of 0.5 and 1.0 P/P_0 suggests the existence of predominant mesopores [30]. At low pressures ($P/P_0 < 0.3$), the uptake of the isotherms for the sample from iodine treatment demonstrates the existence of more micropores than the acid treated sample. The mesopore size distribution determined by BJH is shown in Fig. 5b. The mesopore size distributions of both samples are similar, but the pore volume of the sample purified by iodine treatment is a little larger than that by acid treatment. The reason for this difference might be that Fe particles could not be eliminated completely when boiled in the mixed acid. Fig. 5c illustrates the micropore size distributions obtained from the MP method. From the micropore size distribution, the micropore had a dominant size of about 0.7 nm in the CNCs from iodine treatment. For the CNCs from acid treatment, the pore volume of this size decreased obviously. These results indicate that part of the micropore structure was destroyed during the process of acid treatment. Moreover, if the Fe particles were removed completely under severer conditions, the graphite structure would be damaged further.

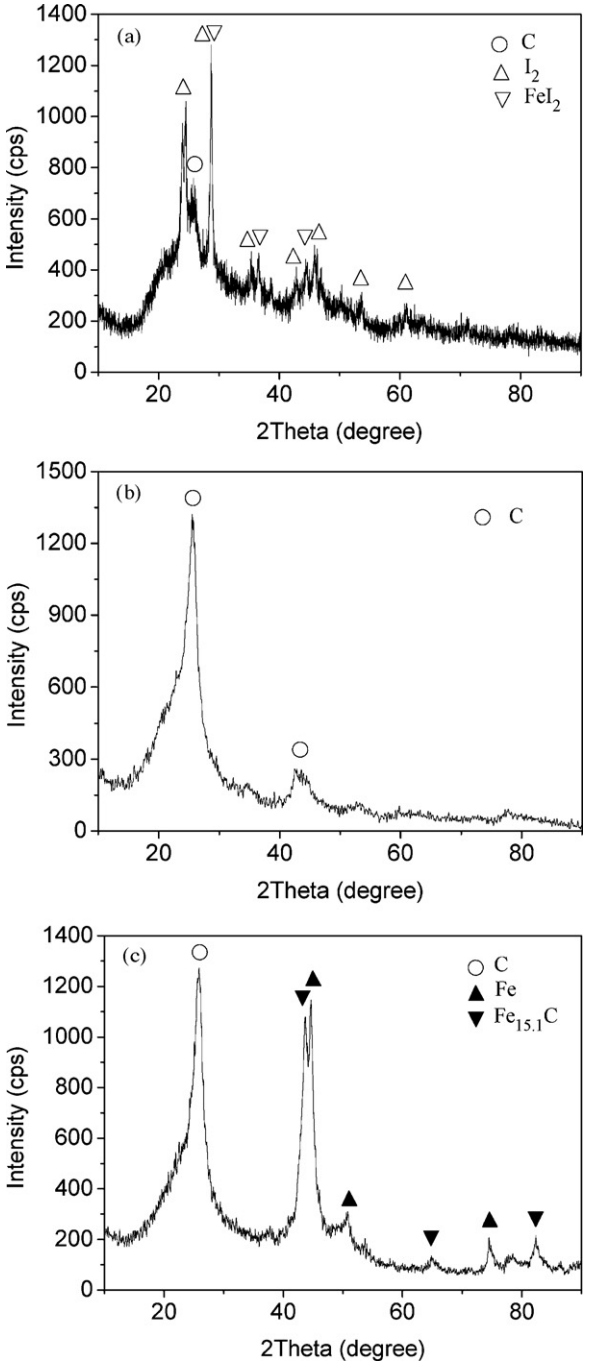

Fig. 2. XRD patterns of CNC samples after heat treatment with iodine (a), after further filtration by ethanol (b), and after direct boiling in mixed acid (c).

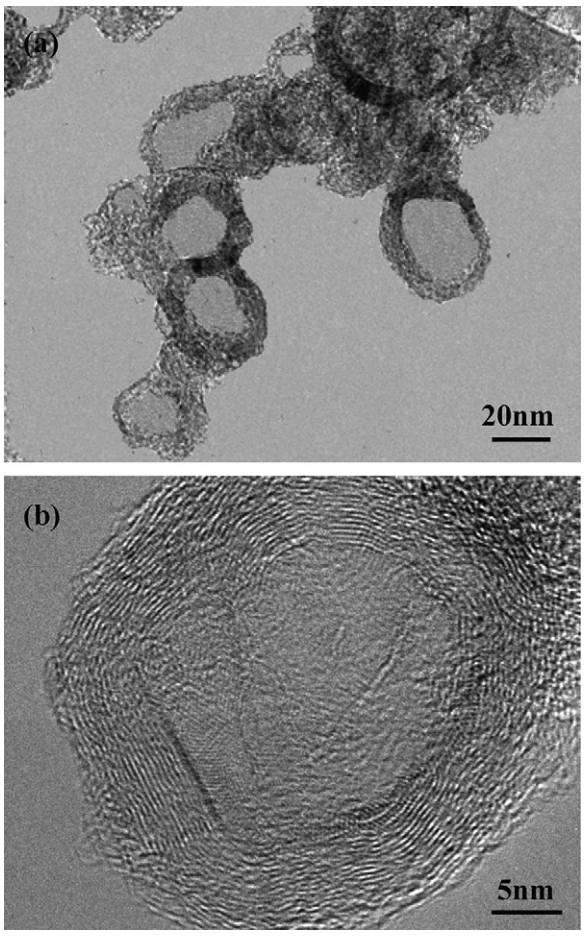

Fig. 3. TEM image (a) and HRTEM image (b) of CNCs after heat treatment with iodine and filtering in ethanol.

3.3. Hollow CNCs as a catalyst support

In order to investigate the performance of the present hollow CNCs as a catalyst support, the hollow CNCs from iodine treatment was studied. An electrochemical study of Pt catalyst (45 wt.%, based on theoretical calculation and determined by thermogravimetry analysis) supported on CNCs (Pt/CNC) was performed. Fig. 6a shows a typical TEM micrograph of the catalyst of Pt/CNC. Pt particles were finely and uniformly dispersed on the CNCs. The HRTEM image (Fig. 6b) shows that the Pt particles are mainly dispersed on the outside of hollow CNCs. Statistic estimation revealed that the average size of the Pt particles on the support was about 3.3 nm. The mean size of the Pt particles was also calculated from the Pt (2 2 0) peak of XRD lines (Fig. 6c) according to the following Scherrer's formula [27]:

$$D = \frac{0.9\lambda_{K\alpha_1}}{\beta_{(2\theta)}\cos\theta_{max}}, \quad (1)$$

where D is the mean size of the Pt particles, $\lambda_{K\alpha_1}$ is the X-ray wavelength (Cu-$\lambda_{K\alpha_1}$ = 0.15418 nm), θ_{max} is the maximum angle of the (2 2 0) peak, and $\beta_{(2\theta)}$ is the half-peak width for Pt (2 2 0) in radian. The value determined from XRD was 3.1 nm, in close agreement with that from TEM images with a deviation no more than 0.2 nm.

Fig. 6d shows the cyclic voltammograms of the catalysts using the different supports. The Pt loading on all supports was 45 wt.%

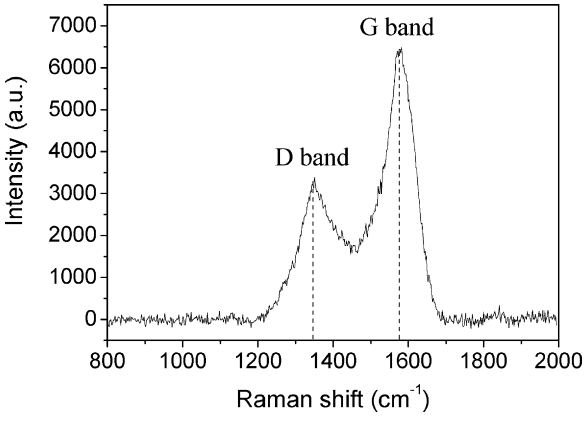

Fig. 4. Raman spectroscopy of the CNCs after heat treatment with iodine.

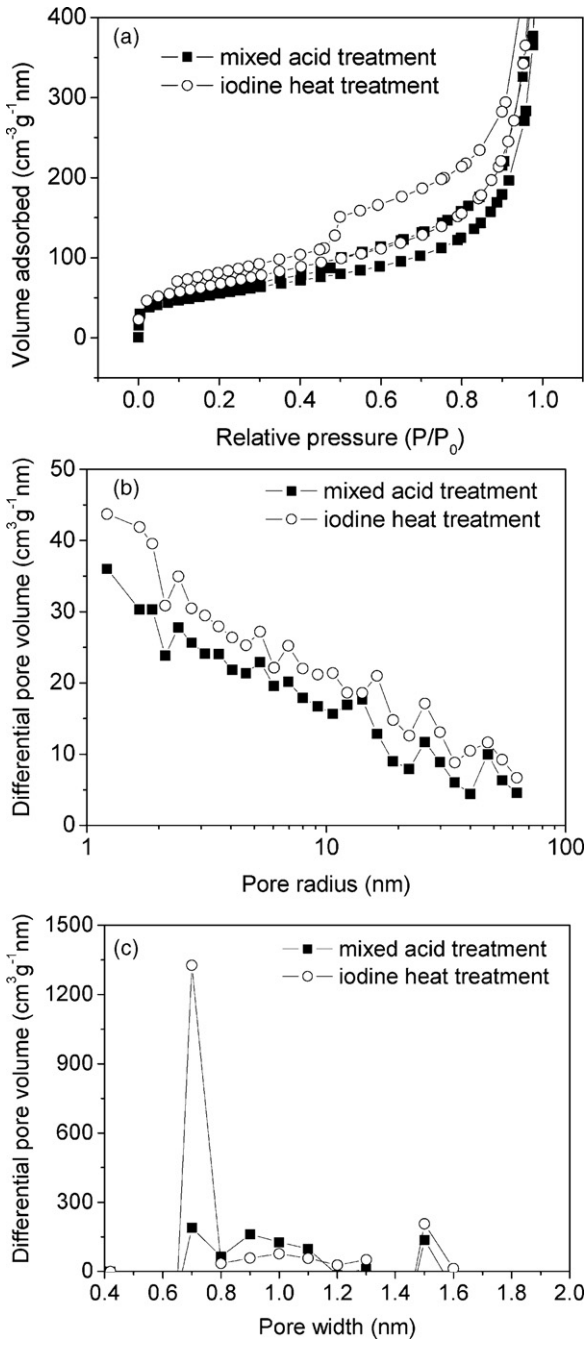

Fig. 5. N_2 adsorption/desorption isotherms (a), mesopore size distribution (b), and micropore size distribution (c) of the CNCs after iodine treatment and acid treatment.

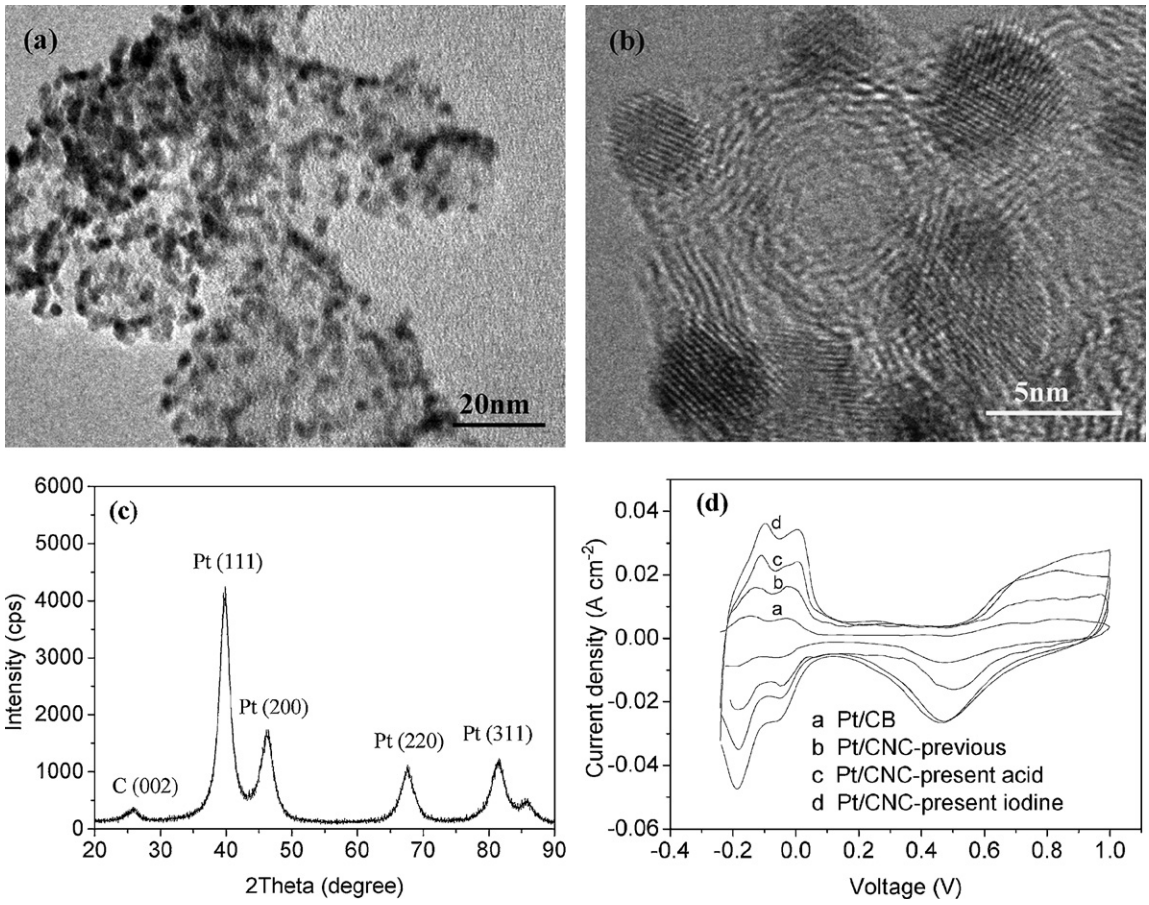

Fig. 6. TEM image (a), HRTEM image (b) and XRD patterns (c) of Pt/CNC; cyclic voltammograms of different catalysts (Pt/CB, Pt/CNC-previous, Pt/CNC-present acid and Pt/CNC-present iodine) (d) (scanning rate 100 mV s^{-1}).

and the amount of Pt on all the electrodes was controlled to be 0.4 mg cm^{-2}. As can be seen, the catalyst supported on the CNCs from iodine treatment (Pt/CNC-present iodine) demonstrates stronger hydrogen desorption and adsorption peaks and thus a higher activity than the catalyst supported on CNCs from acid treatment (Pt/CNC-present acid). When compared with the commercial catalyst supported on conventional carbon black (Pt/CB) and the catalyst we previously reported (Pt/CNC-previous) [10], the present catalyst using CNCs from iodine treatment performed an outstanding electroactivity.

The electroactive surface area for a catalyst can be estimated from the following equation:

$$\alpha = \frac{Q}{m\beta}, \tag{2}$$

where Q is the charge of hydrogen desorption, m is the quantity of Pt used, and β is the charge required to oxidize a monolayer of H_2 on bright Pt (assumed to be 210 μC cm^{-2}). The Q value can be calculated from cyclic voltammogram with taking no account of the contribution of the charge from the electric double layer. The results of effective Q and α are included in Table 1, which suggests that α for the present Pt/CNC catalyst is more than two times higher than the other catalysts.

Table 1
Coulombic charge for hydrogen desorption (Q) and electroactive surface area (α) calculated for different catalysts.

Catalyst	Q [mC cm^{-2}]	α [m^2 g^{-1}]
Pt/CB	13.63	16.23
Pt/CNC-previous	32.42	38.60
Pt/CNC-present acid	40.50	48.21
Pt/CNC-present iodine	70.95	84.46

4. Discussion

The present results expressly reveal that heat treatment with iodine followed by filtration in ethanol is a feasible method to remove the metal particles entrapped in the well-developed graphite shells. In the process of pyrolyzing the mixture of acetylene and iron carbonyl, the decomposition of $Fe(CO)_5$ might have yielded iron nanoparticles that possess a very high catalytic activity for the decomposition of C_2H_2. At high temperature (1300 °C), carbon was produced and dissolved in iron, forming Fe–C intermetallic compounds. Consequently, a thick shell consisting of graphitic layers with a good crystalline structure enwrapped on the surface of the iron particles when the temperature of the particles decreased (Fig. 1b and c). When this iron/graphite core-shell structure with a good crystallinity was boiled in the acid, the entrapped Fe particles could not be eliminated because of the protection of the graphite structure, as shown in Fig. 2b. Moreover, the removal of the Fe particles is at the expense of destroying the graphite layers. Acid oxidized the defective structure in graphite layers first, and then iron particles were dissolved in acid with the destroyed shells left.

Using the iodine treatment method, it is possible to remove the Fe particles enwrapped by thick graphitic shells completely without the destruction of the graphite structure. It has been reported that Fe nanoparticles become unstable when heated at even 250 °C [31]. So the original Fe or Fe–C compound in the core would have a high activity at high temperature. When heated at 1000 °C, Fe atoms would diffuse through structural defects in the graphitic

shells, which were also observed in the previous study [32]. Simultaneously, the outer shell would shrink under thermal irradiation which was proved in situ under electron-beam irradiation [33]. The shrinking of the graphitic shells also promoted outward diffusion of Fe atoms.

When Fe atoms have escaped from the CNCs, it would react immediately with iodine gas existing in the surrounding atmosphere to form iron and iodine compounds (mainly FeI_2 as shown by XRD patterns in Fig. 2a). The reaction can be described approximately as follows:

$$I_2 + Fe \leftrightarrow Fe_xI_y(FeI_2). \quad (3)$$

This is a reversible reaction at high temperature. Owing to the excess of I_2, the reverse reaction hardly occurred. The rightward reaction consumed Fe atoms, resulting in the diffusion of Fe atoms from the cage center. This process would continue until Fe atoms in the core completely vanished, leaving a hollow cage. The reaction products and residual I_2 were removed by dissolving them in ethanol. In this method, Fe atoms diffused outwards through the defective structure in the graphitic shell when heated at high temperature. Therefore, the original graphitic structure was preserved with little damage.

As a support for Pt nanoparticles, the present CNCs from iodine treatment showed better performance than that from acid treatment and previous CNCs and conventional CB. The better performance than that from acid treatment may be related to the presence of more accessible pores which play an important role in oxidation reaction. The apparent improvement than the previous CNCs and conventional CB may be the presence of a better graphitic structure and thus a better conductivity. Besides, the Pt particles supported on the present CNCs exhibited a smaller size (3.3 nm) than those supported on the previous CNCs [10] and CB [34] (>5 nm). This may be another reason for the apparent improvement of electroactive area of Pt on the present CNCs. In addition to the application as a catalyst support, the present CNCs could have many other applications in many areas, such as adsorbents, electrode materials, and energy-storage media [34–39] because they have a unique dimension and structure.

5. Conclusions

In conclusion, iron/graphite core-shell nanoparticles with good graphitization were synthesized by the pyrolysis of acetylene with iron carbonyl. In order to remove the metallic phase at the core, rather than using the conventional acid oxidation, a new method is proposed involving heat treatment with iodine followed by filtration in ethanol. It is found that the iron particles can be completely eliminated and hollow CNCs with good graphitization and high purity can be obtained. The purification mechanism may involve that iron atoms could diffuse out from CNCs and react with iodine molecules in the surrounding atmosphere when the sample is heat treated at high temperature. The reaction product FeI_2 is soluble in ethanol and could be easily removed. When the hollow CNCs are used as a support material for Pt nanoparticles, the Pt/CNC catalyst shows an apparent improvement in the electroactive area. Therefore, the present method could be applied to the production of well-crystallized graphitic carbon in large scale. The resultant CNCs could prove to be practically relevant for fuel cell and many other technologies.

Acknowledgements

J.N. Wang is thankful to the research fund (project # 50871067) from the National Natural Science Foundation of China and the fund for the national 863 project of 2007AA05Z128 from the Ministry of Science and Technology of China.

References

[1] R. Ryoo, S.H. Joo, S. Jun, J. Phys. Chem. B 103 (1999) 7743–7746.
[2] A.-H. Lu, W. Schmidt, N. Matoussevitch, H. Bönnermann, B. Spliethoff, B. Tesche, E. Bill, W. Kiefer, F. Schuth, Angew. Chem. Int. Ed. 43 (2004) 4303–4306.
[3] B.E.I. Hamaoui, L. Zhi, J. Wu, U. Kolb, K. Müllen, Adv. Mater. 17 (2005) 2957–2960.
[4] D.M. Gattia, M.V. Antisari, L. Giorgi, R. Marazzi, E. Piscopiello, A. Montone, S. Bellitto, S. Licoccia, E. Traversa, J. Power Sources 194 (2009) 243–251.
[5] P.V. Shanahan, L.B. Xu, C.D. Liang, M. Waje, S. Dai, Y.S. Yan, J. Power Sources 185 (2009) 423–427.
[6] D. Bom, R. Andrews, D. Jacques, J. Anthony, B. Chen, M.S. Meier, J.P. Selegue, Nano Lett. 2 (2002) 615–619.
[7] J.J. Wang, G.P. Yin, Y.Y. Shao, Z.B. Wang, Y.Z. Gao, J. Phys. Chem. C 112 (2008) 5784–5789.
[8] J.N. Wang, Y.Z. Zhao, J.J. Niu, J. Mater. Chem. 17 (2007) 2251–2256.
[9] Z.M. Sheng, J.N. Wang, Adv. Mater. 20 (2008) 1071–1075.
[10] B.Y. Xia, J.N. Wang, X.X. Wang, J.J. Niu, Z.M. Sheng, M.R. Hu, Q.C. Yu, Adv. Funct. Mater. 18 (2008) 1790–1799.
[11] J.J. Niu, J.N. Wang, L. Zhang, Y.Q. Shi, J. Phys. Chem. C 111 (2007) 10329–10335.
[12] T. Oku, I. Narita, A. Nishiwaki, Diamond Relat. Mater. 13 (2004) 1337–1341.
[13] Y.W. Ma, Z. Hu, K.F. Huo, Y.N. Lu, Y.M. Hu, Y. Liu, J.H. Hu, Y. Chen, Carbon 43 (2005) 1667–1672.
[14] T. Oku, T. Hirano, K. Suganuma, S. Nakajima, Mater. Res. Soc. 14 (1999) 4266–4273.
[15] N. Sano, H. Wang, M. Chhowalla, I. Alexandrou, G.A.J. Amaratunga, Nature 414 (2001) 506–507.
[16] K. Hernadi, A. Siska, L. Thiên-Nga, L. Forró, I. Kiricsi, Solid State Ionics 203 (2001) 141–142.
[17] J.-F. Colomer, P. Pierdigrosso, A. Fonseca, J.B. Nagy, Synth. Met. 103 (1999) 2482–2483.
[18] A. Fonseca, K. Hernadi, J.B. Nagy, D. Bernaerts, A.A. Lucas, J. Mol. Catal. 107 (1996) 159–168.
[19] X.C. Chen, C.S. Chen, Q. Chen, F.Q. Cheng, G. Zhang, Z.Z. Chen, Mater. Lett. 57 (2002) 734–738.
[20] K. Hernadi, A. Fonseca, J.B. Nagy, D. Bernaerts, J. Riga, A. Lucas, Synth. Met. 77 (1996) 31–34.
[21] M. Holzinger, A. Hirsch, P. Bernier, G.S. Duesberg, M. Burghard, Appl. Phys. A 70 (2000) 599–602.
[22] T.W. Ebbesen, P.M. Ajayan, H. Hiura, K. Tanigaki, Nature 367 (1994) 519–1519.
[23] A.G. Rinzler, J. Liu, H. Dai, P. Nikolaev, C.B. Huffmann, F.J. Rodriguez-Macias, P.J. Boul, A.H. Lu, D. Heymann, D.T. Colbert, R.S. Lee, J.E. Fisher, A.M. Rao, P.C. Eklund, R.E. Smalley, Appl. Phys. A 67 (1998) 29–37.
[24] M. Ginic-Markovic, J.G. Matisons, R. Cervini, G.P. Simon, P.M. Fredericks, Chem. Mater. 18 (2006) 6258–6262.
[25] F. Tuinstra, J.L. Koenig, J. Chem. Phys. 53 (1970) 1126–1130.
[26] R.J. Nemanich, S.A. Solin, Phys. Rev. B 20 (1979) 392–401.
[27] V. Radmilovic, H.A. Gasteiger, P.N. Ross, J. Catal. 154 (1995) 98–106.
[28] S.H. Joo, C. Pak, D.J. You, S.A. Lee, H.I. Lee, J.M. Kim, H. Chang, D. Seung, Electrochim. Acta 52 (2006) 1618–1626.
[29] S.S. Kim, T.R. Pauly, T.J. Pinnavaia, Chem. Commun. 17 (2000) 1661–1662.
[30] S.J. Gregg, K.S.W. Sing, Adsorption, Surface Area and Porosity, 2nd ed., Academic Press, London, 1982.
[31] G. Liu, B.X. Qin, Y.B. Guo, R.H. Fan, N. Lu, Ordnance Mater. Sci. Eng. 26 (2003) 18–22.
[32] Z.M. Sheng, J.N. Wang, Carbon 44 (2006) 2098–2101.
[33] F. Banhart, Rep. Prog. Phys. 62 (1999) 1181–1221.
[34] J.N. Wang, L. Zhang, J.J. Niu, F. Yu, Z.M. Sheng, Y.Z. Zhao, H. Chang, C. Pak, Chem. Mater. 19 (2007) 453–459.
[35] R.W. Fu, T.F. Baumann, S. Cronin, G. Dresselhaus, M.S. Dresselhaus, J.H. Satcher Jr., Langmuir 21 (2005) 2647–2651.
[36] T. Hyeon, S. Han, Y.-E. Sung, K.-W. Park, Y.-W. Kim, Angew. Chem. Int. Ed. 42 (2003) 4352–4356.
[37] S. Han, Y. Yun, K.-W. Park, Y.-E. Sung, T. Hyeon, Adv. Mater. 15 (2003) 1922–1925.
[38] A.-H. Lu, W.-C. Li, N. Matoussevitch, B. Spliethoff, H. Bönnermann, F. Schüth, Chem. Commun. 1 (2005) 98–100.
[39] A.-H. Lu, W.-C. Li, E.-L. Salabas, B. Spliethoff, F. Schüth, Chem. Mater. 18 (2006) 2086–2094.